UNIVERSITÄT
BAYREUTH

Master Thesis

Stabilizing Global Simulation in GKW by the Introduction of the Parallel Electric Field $E_{\parallel}$

Manuel Lippert

Submission date: January 4, 2024

Physics Department at the University of Bayreuth

Supervisors:
Prof. Arthur G. Peeters
Dr. Florian Rath

★ 07.07.2020

This thesis is dedicated to my cat **Leo**
who is part of our family since July 2020.
He is the kindest cat I ever own and very playful.
For a long life together.

I love you.

Manuel Lippert
January 4, 2024

Contents

CHAPTER

1

Motivation

Ion temperature gradient driven turbulence close to marginal stability exhibits zonal flow pattern formation on mesoscales, so-called $\mathrm{E}\times\mathrm{B}$ staircase structures[5]. Such pattern formation has been observed in local gradient-driven flux-tube simulations[13,15], including collisions[22] and background $\mathrm{E}\times\mathrm{B}$ shear[15], local flux-driven realizations including mean electric field shear[16], as well as global gradient-driven[12,20,17] and global flux-driven[5,6,21,8,9] studies. In global studies, spanning a larger fraction of the minor radius, multiple radial repetitions of staircase structures are usually observed, with a typical pattern size of several ten Larmor radii. By contrast, in the aforementioned local studies the radial size of $\mathrm{E}\times\mathrm{B}$ staircase structures is always found to converge to the radial box size of the flux tube domain. The above observations lead to the question:

Does the basic pattern size always converges to the box size, or is there a typical mesoscale size inherent to staircase structures also in a local flux-tube description?

The latter case would imply that it is not necessarily global physics, i.e., profile effects, that set

(i) the radial size of the $\mathrm{E}\times\mathrm{B}$ staircase pattern

(ii) the scale of avalanche-like transport events.

These transport events are usually restricted to $\mathrm{E}\times\mathrm{B}$ staircase structures and considered as a nonlocal transport mechanism[5].

In this bachlor thesis the above question is addressed through a box size convergence scan of the same cases close to the nonlinear threshold for turbulence generation as studied in Ref. 13.

CHAPTER

2

Plasma Physics Basics

2.1 Charged Particle Motion in Magnetic and Electric Field

In magnetic confinement devices like the tokamak reactor, the charged particles experience forces caused by magnetic and electric fields which results in distinct motion under the associated force. Charged particles can be separated in species, e.g. electrons and ions, which will be later on not displayed in the governing equation. Throughout this thesis the charge q, the mass m or the temperature T indicate the quantities of a specific species, i.e., electrons or ions.

2.1.1 Particle Motion perpendicular to the magnetic field

Due to the Lorentz force, particles with a velocity component perpendicular to the homogenous magnetic field $v_\perp$ undergo a circular motion in the plane perpendicular to the magnetic field [Fig. 2.1(a)]. This type of motion has circular frequency, which is often referred to as *cyclotron frequency* and is defined as

$$\omega_\mathrm{c} = \frac{|q|B}{m} \ , \tag{1}$$

where m and q are the mass and the charge of the particle and B the strength of the magnetic field. The radius, the so called *Larmor radius*, of this motion is given by

$$\rho = \frac{mv_\perp}{|q|B} \tag{2}$$

with the center often being referred to as *gyrocenter*. Note that since the Lorentz force depends on the species charge of the particle, the circulation direction is the opposite between electron in ions.

Due to Coulomb collisions the plasma gets thermalized. Together with the Maxwell-Boltzmann distribution the typical thermal velocity is

$$v_\mathrm{th} = \sqrt{\frac{2T}{m}} \ , \tag{3}$$

where T represents the species temperature. Based on the thermal velocity v_th the *thermal Larmor radius* gets introduced as[23]

$$\rho_\mathrm{th} = \frac{mv_\mathrm{th}}{|q|B} \ . \tag{4}$$

2.1.2 Particle Motion parallel to the magnetic field

In absence of forces in the direction parallel to the magnetic field the particles can move freely in parallel direction to the homogenous magnetic field. The velocity of this motion is of order of the thermal velocity v_{th} and is dominated by electrons due to their lighter mass compared to ions ($v_{\mathrm{th,e}}/v_{\mathrm{th,i}} = 60$).

When an electric field with a component parallel to the magnetic field $E_{\parallel}$ influences the plasma the charged particles are accelerated by the electric force

$$F_{\parallel,E} = qE_{\parallel} \ . \tag{5}$$

The parallel motion follows then from the equation of motion. Here the direction of the motion also depends on the species type [Fig. 2.1(b)].

Since magnetic fields are not always homogenous, an inhomogeneous magnetic field with its gradient ∇B containing a component parallel to the magnetic field which is given by

$$\nabla_{\parallel} B = \frac{\mathbf{B}}{B} \cdot \nabla B \tag{6}$$

causes the force

$$F_{\parallel,\nabla_{\parallel}B} = -\frac{mv_{\perp}^2}{2B}\nabla_{\parallel}B = -\mu\nabla_{\parallel}B \ ; \qquad \mu = \frac{mv_{\perp}^2}{2B} \tag{7}$$

with *magnetic moment* μ. The magnetic moment μ is an adabatic invariant (constant of motion) if the variation of the magnetic field over time is smaller than the inverse of the cyclotron frequency ω_{c}^{-1} and the spatial variation is larger the Larmor radius ρ_{L}. The resulting force has its application in the mirror effect where a charged particle gets reflected due to this force [Fig. 2.1(c)].[23]

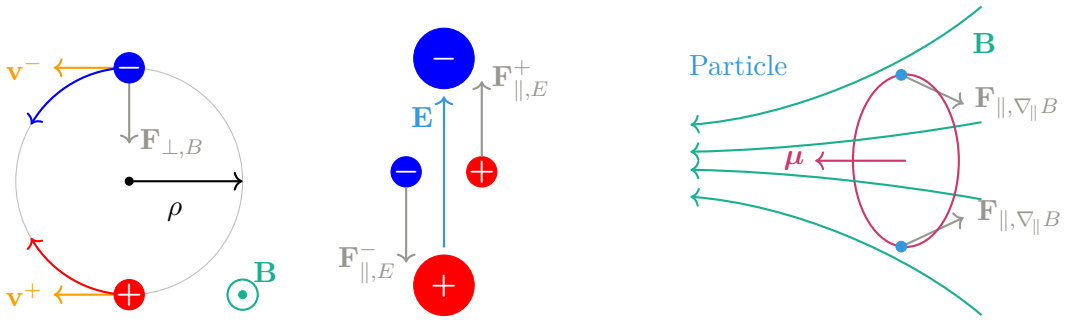

(a) **(b)** **(c)**

Figure 2.1: Forces acting on a charged particle:
(a) Lorentz force $\mathbf{F}_{\perp,B}$ perpendicular to velocity $\mathbf{v}^{\pm}$ and magnetic field $\mathbf{B}$ which causes, circular motion with different directions for electron and ions, Lamor radius ρ_{L} and cyclotron frequency ω_{c},
(b) Electric force $\mathbf{F}^{\pm}_{\parallel,E}$ with electric field $\mathbf{E}$,
(c) Mirror effect with force $\mathbf{F}_{\parallel,\nabla_{\parallel}B}$ and magnetic moment μ caused by an inhomogeneous magnetic field $\mathbf{B}$.

2.1.3 Drifts in the Gyrocenter

In the presence of a magnetic field (homogenous, inhomogeneous or perturbed) and electric fields the gyrocenter undergoes slow (compared to the thermal velocity v_{th}) drift motions perpendicular to the magnetic field. There are several examples for this drift motion. According to this thesis topic only the main three drift types will be covered in the following.

1. **E × B Drift:**
   If an electric field **E** with a perpendicular component together with the magnetic field **B** (both fields are homogenous) is present the acting Coulomb force and Lorentz force results into a drift of the gyrocenter with

$$\mathbf{v}_E = \frac{\mathbf{E} \times \mathbf{B}}{B^2} \tag{8}$$

   which is called the E × B drift. Since both acting forces direction depends on the species type the direction of the E × B drift is for every species the same [Fig. 2.2(a)].

2. **∇B Drift:**
   Inhomogeneous magnetic field causes a gradient ∇B of the magnetic field. Because of that gradient the gyrocenter undergoes a ∇B drift defined by

$$\mathbf{v}_{\nabla B} = \frac{m v_\perp^2}{2q} \frac{\mathbf{B} \times \nabla B}{B^3} \ . \tag{9}$$

   The gradient of the magnetic field ∇B varies thereby on scales larger compared to the Larmor radius. The direction of the ∇B drift depends on the species type [Fig. 2.2(b)].

3. **Curvature Drift:**
   Due to centrifugal force acting on the particle in a curved magnetic field the gyrocenter experiences a curvature drift according to

$$\mathbf{v}_C = \frac{m v_\parallel^2}{q} \frac{\mathbf{B} \times \mathbf{C}}{B^2} = \frac{m v_\parallel^2}{q} \frac{\mathbf{B} \times \nabla B}{B^3} \ ; \qquad \mathbf{C} = -(\mathbf{b} \cdot \nabla)\mathbf{b} = \frac{\nabla B}{B} \ , \tag{10}$$

   where **b** is the unit vector along the magnetic field. To obtain the result for the curvature **C** in Eq. (10) the plasma pressure has to be small compared to the magnetic field strength B. In the form of Eq. (10) ∇B and curvature drift can be treated similarly.[23]

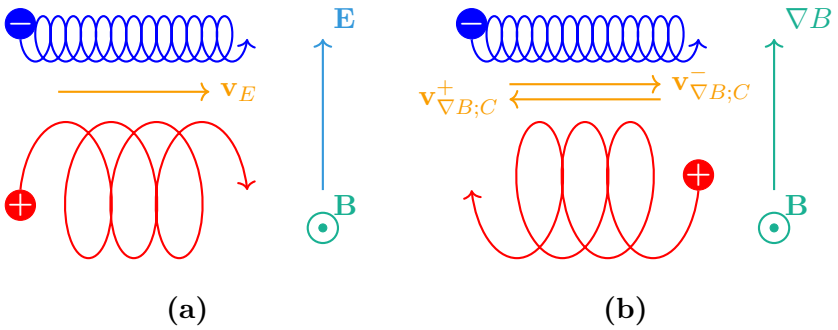

Figure 2.2: Dirft motion in gyrocenter:
(a) E × B Drift with drift velocity $\mathbf{v}_E$, electric field **E** and magnetic field **B**,
(b) ∇B Drift/Curvature Drift with drift velocity $\mathbf{v}^{\pm}_{\nabla B;\kappa}$, magnetic field **B** and gradient of the magnetic field ∇B.

2.2 Magnetic Confinement and Plasma Rotation

In tokamak devices strong magnetic fields confine the hot plasma. As mentioned in Chapter 2.1 a magnetic field forces a perpendicular particle motion and a motion which contains the gyro motion and slow perpendicular gyro center drifts. Because of the much smaller size of the Larmor radius compared to the device size R the particle and energy losses are caused by the gyro center drift. To avoid additional loss of particles because of the parallel motion the field lines of the magnetic field in the tokamak devices is shaped like a torus. This type of geometry has nested surfaces with constant magnetic flux, so-called *flux surfaces*, and magnetic field lines which lie on these surfaces. To maintain stability the magnetic field has a toroidal and a poloidal component. According to the force balance the magnetic field is equivalent to the plasma pressure which means on flux-surfaces the plasma pressure is constant.[18,23] The toroidal component is produced by external coils whereas the poloidal component is provided by the toroidal plasma current. Together the components result in a magnetic field which follows helical trajectories [Fig 2.3]. To characterize the quality of confinement the so-called *plasma beta* is used and is given as

$$\beta = \frac{nT}{\mu_0 B^2/2} \ , \tag{11}$$

with n the plasma density, T as temperature, μ_0 the permeability in vacuum and the magnetic field strength B. Respectively, the plasma beta compares the thermal plasma pressure nT to the ambient magnetic field pressure $\mu_0 B^2/2$. For fusion devices the plasma beta has to be a bit smaller than 1 ($\beta < 1$) for optimal confinement. In a tokamak reactor the plasma beta has a typical order of a few percent.[23]

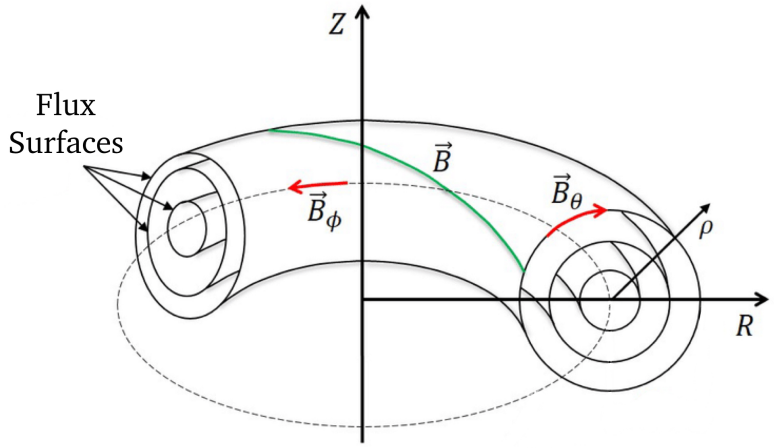

Figure 2.3: Toroidal flux surfaces in tokamak plasma with helical magnetic field (green line) in torus coordinates (ρ (radial), ϕ (toroidal), θ (poloidal)) or cylindrical coordinates (Z, R, ϕ).[1]

The rotation of the plasma can be described in a co-rotating frame of reference, which is rigidly rotating with the velocity $\mathbf{u}_0$ and will be used later on in the derivation of the gyrokinetic equations in Chapter 3.2. It assumend that the poloidal component of the plasma rotation is much smaller compared to the toridial component and will be neglected. With this assumption in mind the reference frame is chosen to move in the toridial direction exclusivly and its velocity $\mathbf{u}_0$ can be expressed as

$$\mathbf{u}_0 = \mathbf{\Omega} \times \mathbf{x} = R^2 \Omega \nabla \varphi \ , \tag{12}$$

where $\mathbf{\Omega}$ is the constant angular frequency, φ is the toroidal angle and $R\nabla\varphi$ is the unit vector in the toroidal direction. Since the rotation of the plasma in the labortory frame is not a rigid body rotation, it will be characterized by the radial profile of the angular velocity $\hat{\Omega}(\psi)$. Then the angular frequency of the rotating frame Ω is chosen to match the the plasma rotation on a certain point, i.e. $\Omega = \hat{\Omega}(\psi_r)$. The plasma rotation in the co-rotating frame of reference will be denoted as

$$\omega_\varphi(\psi) = \hat{\Omega}(\psi) - \Omega. \tag{13}$$

with the rotation speed along the magnetic field line

$$u_\parallel = \frac{RB_\mathrm{t}}{B} \omega_\varphi(\psi) \ , \tag{14}$$

where B_t is the toridial component of the magnetic field.[14]

CHAPTER

Derivation of Gyrokinetic Equation

3

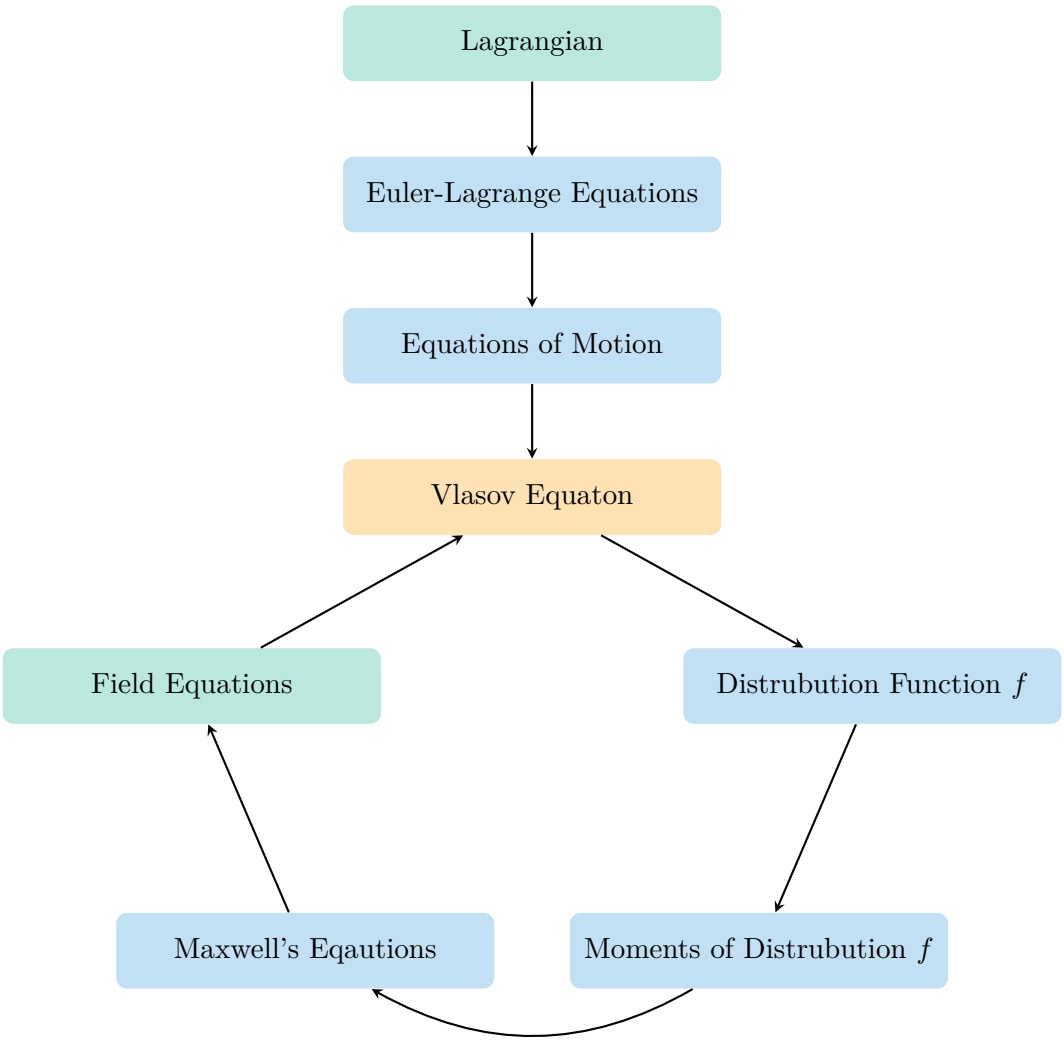

Figure 3.1: Iterative Solution of the Vlasov Maxwell system in Lagrangian formalism

3.1 Gyrokinetic Ordering

In the derivation of the gyrokinetic theory the aim is to decouple the effect of small-scale, small amplitude fluctuations of the plasma in the Langrangian. For this it is chosen to take the properties of fluctuations as small parameter, which will get in the ordering assumptions applied in gyrokinetic theory[2]

$$\begin{aligned} \frac{|\mathbf{A_1}|}{|\mathbf{A_0}|} &\sim \frac{\Phi_1}{\Phi_0} \sim \epsilon_\delta \ll 1 \\ \rho\frac{\nabla B_0}{B_0} &\sim \rho\frac{\nabla E_0}{E_0} \sim \frac{\rho}{L_B} \sim \epsilon_B \ll 1 \\ k_\perp \rho &\sim \epsilon_\perp \sim 1 \\ \frac{\omega}{\omega_\mathrm{c}} &\sim \epsilon_\omega \ll 1 \end{aligned} \tag{1}$$

where $\mathbf{A}$ and Φ are the vector and scalar potentials, $\mathbf{B}$ and $\mathbf{E}$ are the magnetic and electric fields, ω and $k_\perp$ are the typical mode frequency and perpendicular wavenumber defined as $k_\perp = |\mathbf{k} \times \mathbf{b}|$, ρ and ω_c are the Larmor radius and cyclotron frequency and L_B the equilibrium magnetic length scale. The equilibrium quantities are denoted with 0 and the fluctuations with 1 subscript.

The above-mentioned equations state that fluctuations have a much smaller magnitude than the corresponding equilibrium values, their typical timescale is much slower than the Larmor frequency, their characteristic length scale is of the order of the Larmor radius, and it is typically much shorter the equilibrium spatial variation scale. Teh gyrokinetic equations are valid under these ordering assumptions.

The small parameters ϵ_δ, ϵ_B, $\epsilon_\perp$ and ϵ_ω are due to different physical but in practice it is assumed that they are of simular order and substitute them with one parameter. For the derivation of the gyrokinetic equations of GKW all derived equations are evaluated up to the first order of the ratio of the reference thermal Larmor radius $\rho_{\mathrm{th,ref}}$ and the equilibrium magnetic length scale L_B as small parameter and is defined as[19]

$$\rho_\star = \frac{\rho_{\mathrm{th,ref}}}{L_B} = \frac{m_{\mathrm{ref}} v_{\mathrm{th,ref}}}{e B_{\mathrm{ref}}} \sim \epsilon_B \sim \epsilon_\delta \sim \epsilon_\omega \ . \tag{2}$$

3.2 Gyrokinetic Lagrangian (Fundamental One-Form)

3.2.1 Lagrangian in Patricle Phase Space

The Lagrangian of a particle γ with mass m and charge number Z in the electro magnetic field will be described through the particle position $\mathbf{x}$ and the velocity $\mathbf{v}$ as coordinates $\{\mathbf{x}, \mathbf{v}\}$ and can be written as

$$\gamma = \gamma_\nu \mathrm{d}z^\nu = \underbrace{(m\mathbf{v} + Ze\mathbf{A}(\mathbf{x}))}_{\text{Sympletic Part}} \cdot \mathrm{d}\mathbf{x} - \underbrace{\left(\frac{1}{2}mv^2 + Ze\Phi(\mathbf{x})\right)}_{\text{Hamiltonian } H(\mathbf{x},\mathbf{v})} \mathrm{d}t \ , \tag{3}$$

where $\mathbf{A}$ and Φ are the vector and scalar potential, ν indexes the six coordinates, and Einstein notation is applied. This form is also known as fundamental one-form.

The defined Lagrangian γ will then be transformed in the rotating frame of reference [Ch. 2.2], which can be achieved the following Lorentz transformation

$$\mathbf{v} \to \mathbf{v} + \mathbf{u}_0 \qquad \mathbf{E} \to \mathbf{E} + \mathbf{u}_0 \times \mathbf{B} \qquad \Phi \to \Phi + \mathbf{A} \cdot \mathbf{u}_0 \ . \tag{4}$$

After performing the transformation outlined in Ref. 14 the Lagrangian γ becomes

$$\gamma = (m\mathbf{v} + m\mathbf{u}_0 + Ze\mathbf{A}(\mathbf{x})) \cdot \mathrm{d}\mathbf{x} - \left(\frac{1}{2}mv^2 - \frac{1}{2}mu_0^2 + Ze\Phi(\mathbf{x})\right) \mathrm{d}t \ . \tag{5}$$

In the next step small scale perturbations of the electromagnetic field gets introduced as following

$$\mathbf{A} = \mathbf{A}_0 + \mathbf{A}_1 \qquad \Phi = \Phi_0 + \Phi_1 \ . \tag{6}$$

Here, it is assumend that the equilibrium electric field is zero in a stationary plasma, but it will be kept in case for finite plasma rotation. According to the gyrokinetic ordering [Ch. 3.1] the perturbations are in the first order of $\rho_\star$. Taking everything into account the Lagrangian in the particle phase space with perturbations can be written as

$$\begin{aligned} \gamma &= \gamma_0 + \gamma_1 \\ \gamma_0 &= (m\mathbf{v} + m\mathbf{u}_0 + Ze\mathbf{A}_0(\mathbf{x})) \cdot \mathrm{d}\mathbf{x} - \left(\frac{1}{2}mv^2 - \frac{1}{2}mu_0^2 + Ze\Phi_0(\mathbf{x})\right) \mathrm{d}t \\ \gamma_1 &= Ze\mathbf{A}_1(\mathbf{x}) \cdot \mathrm{d}\mathbf{x} - Ze\Phi_1(\mathbf{x}) \, \mathrm{d}t \ . \end{aligned} \tag{7}$$

3.2.2 Lagrangian in Guiding Center Phase Space

For the description of charged particle behaviour in the tokamak device the *guiding center coordinates* are used [Fig. 3.2]. This set of coordinates are defined as the following

$$\begin{aligned} \mathbf{X}(\mathbf{x},\mathbf{v}) &= \mathbf{x} - \rho(\mathbf{x},\mathbf{v})\mathbf{a}(\mathbf{x},\mathbf{v}) & v_\parallel &= \mathbf{v}\cdot\mathbf{b}(\mathbf{x}) \\ \mu(\mathbf{x},\mathbf{v}) &= \frac{m v_\perp^2(\mathbf{x})}{2B(\mathbf{x})} & \theta(\mathbf{x},\mathbf{v}) &= \arccos\left(\frac{1}{v_\perp}\left(\mathbf{b}(\mathbf{x})\times\mathbf{v}\right)\cdot\hat{\mathbf{e}}_1\right) , \end{aligned} \tag{8}$$

where the guiding center follows the magnetic field with the parallel velocity $v_\parallel$. The gyromotion is described together with the magnetic moment μ, the guiding center $\mathbf{X}$ and the gyro phase θ which gives a parameter set of six quantities $\{\mathbf{X}, v_\parallel, \mu, \theta\}$. Vector $\mathbf{b}(\mathbf{x})$ is the unit vector in the direction of the equilibrium magnetic field and $\rho(\mathbf{x},\mathbf{v})\mathbf{a}(\mathbf{x},\mathbf{v})$ is the vector pointing from the guiding center to the particles postion, which is defined by the unit vector $\mathbf{a}(\mathbf{x},\mathbf{v})$ and its length is the Lamor radius $\rho(\mathbf{x},\mathbf{v})$. The unit vector $\mathbf{a}(\mathbf{x},\mathbf{v})$ can be expressed in a local orthonormal basis as the function of the gyroangle θ

$$\mathbf{a}(\theta) = \hat{\mathbf{e}}_1\cos\theta + \hat{\mathbf{e}}_2\sin\theta \ . \tag{9}$$

The vectors $\mathbf{b}$, $\hat{\mathbf{e}}_1$ and $\hat{\mathbf{e}}_2$ form a local Cartesian coordinate system at the guiding center position.

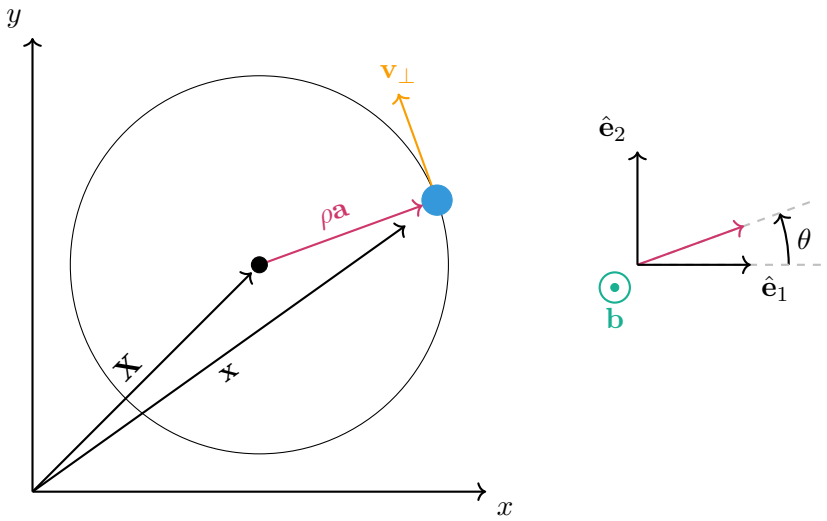

Figure 3.2: Sketch of guiding center coordinates where the charged particle performs a circular motion around the guiding center.[11]

To transform the fundamental one-from into the guiding center coordinates the following relation will be used

$$\Gamma_\eta = \gamma_\nu \frac{\mathrm{d}z^\nu}{\mathrm{d}Z^\eta} \ , \tag{10}$$

where Γ_η is a component of the guiding center fundamental one-form. To calculate the new coordinates the transformation [Eq. (8)] have to be inverted to provide the old coordinates as function of the new one $z(Z)$. Here, the direct transformation is clearly uniquely determined if the magnetic field is known at the particle postion. However, the inverse transformation is not uniquely due to the dependence of the Larmor radius ρ on magnetic field at the particle position $\mathbf{x}$. Taylor expansion of the Larmor radius ρ around the guiding center $\mathbf{X}$ yields $\rho(\mathbf{x}) \approx \rho(\mathbf{X})$. Note, that terms of order ρ^2, which leads to second order terms in $\rho_\star$, will get neglected due to the gyrokinetic ordering. The Larmor radius ρ also depends on the velocity $\mathbf{v}$ in particle phase space [Eq. (2)], or the magnetic moment μ in the guiding center phase space through the formular

$$\rho(\mathbf{X}, \mu) = \frac{1}{Ze}\sqrt{\frac{2\mu m}{B(\mathbf{X})}} \ . \tag{11}$$

This dependence will be only used if greater clarity is needed. With result of the taylor expansion the particle position $\mathbf{x}$ can be expressed with the guiding center coordinates as

$$\mathbf{x}(\mathbf{X}, \theta) \approx \mathbf{X} + \rho(\mathbf{X})\mathbf{a}(\theta) \ . \tag{12}$$

The particle velocity $\mathbf{v}$ is the sum of the velocity along the magnetic field $v_\parallel$, the gyration velocity $\mathbf{v}_\perp$ and the drift velocity, which will be neglected because the particle drifts can be described by the motion of the guiding center. So to summarize the velocity $\mathbf{v}$ in the guiding center frame can be expressed as

$$\mathbf{v} = v_\parallel \mathbf{b}(\mathbf{x}) + \mathbf{v}_\perp = v_\parallel \mathbf{b}(\mathbf{x}) + \rho(\mathbf{x})\dot{\mathbf{a}}(\theta) \ . \tag{13}$$

Applying Taylor expansion again around the guding center $\mathbf{X}$ teh following expression can be obtained

$$\mathbf{v}(\mathbf{X}, v_\parallel, \mu, \theta) \approx v_\parallel \left[\mathbf{b}(\mathbf{X}) + \partial_{\mathbf{X}}\mathbf{b}(\mathbf{X}) \cdot \mathbf{a}(\theta)\rho(\mathbf{X}, \mu)\right] + \rho(\mathbf{X}, \mu)\dot{\mathbf{a}}(\theta) \ . \tag{14}$$

Now, the transformation [Eq. (10)] can be applied to express the fundamental one-form in the new coordinates with the following components

$$\begin{aligned}
\Gamma_{X^i} &= \gamma_{x^j}\frac{\mathrm{d}x^j}{\mathrm{d}X^i} + \gamma_{v^j}\frac{\mathrm{d}v^j}{\mathrm{d}X^i} + \gamma_t\frac{\mathrm{d}t}{\mathrm{d}X^i} = \gamma_{x^j}\frac{\mathrm{d}x^j}{\mathrm{d}X^i} & \Gamma_{v_\parallel} &= \gamma_{x^j}\frac{\mathrm{d}x^j}{\mathrm{d}v_\parallel} + \gamma_{v^j}\frac{\mathrm{d}v^j}{\mathrm{d}v_\parallel} = 0 \\
\Gamma_\mu &= \gamma_{x^j}\frac{\mathrm{d}x^j}{\mathrm{d}\mu} & \Gamma_\theta &= \gamma_{x^j}\frac{\mathrm{d}x^j}{\mathrm{d}\theta} \\
\Gamma_t &= \gamma_t\frac{\mathrm{d}t}{\mathrm{d}t} + \mu B(\mathbf{X}) = \gamma_t + \mu B(\mathbf{X}) \ .
\end{aligned} \tag{15}$$

Note, that to the Hamiltonian part Γ_t the energy term of the magnetic field B at the guiding center $\mathbf{X}$ has to be added, due to the circular motion of the particle around the center.

In Equation (15) the components of the fundamental one-form of the particle phase space γ_ν and the equation for $\mathbf{v}$ in guiding center coordinates [Eq. (14)] will be inserted and the Taylor expansion up to the first order applied for terms containing the particle position $\mathbf{x}$ as argument. After that the gyroaveraging operator will be used, which is defined as the integral over the gyrophase θ

$$\langle \cdot \rangle = \frac{1}{2\pi} \int_0^{2\pi} (\cdot) \, \mathrm{d}\theta \ . \tag{16}$$

Due to the definition of the vector $\mathbf{a}$ [Eq. (9)] the first order terms in $\mathbf{a}$ and $\dot{\mathbf{a}}$ disappear under gyroaveraging. Following all the previous steps, one can obtain

$$\begin{aligned} \langle \Gamma_{\mathbf{X}} \rangle &= m v_\parallel b_i(\mathbf{X}) + m u_{0i} + Ze\mathbf{A}(\mathbf{X}) & \langle \Gamma_{v_\parallel} \rangle &= 0 \\ \langle \Gamma_\mu \rangle &= 0 & \langle \Gamma_\theta \rangle &= \frac{2\mu m}{Ze} \\ \langle \Gamma_t \rangle &= -\left(\frac{1}{2} m v_\parallel^2 - \frac{1}{2} m u_0^2 + Ze\Phi(\mathbf{X}) + \mu B(\mathbf{X}) \right) \ , \end{aligned} \tag{17}$$

which results in the fundamental one-form in guiding center coordinates

$$\begin{aligned} \langle \Gamma \rangle = &\left(m v_\parallel \mathbf{b}(\mathbf{X}) + m\mathbf{u}_0 + Ze\mathbf{A}(\mathbf{X}) \right) \cdot \mathrm{d}\mathbf{X} + \frac{2\mu m}{Ze} \mathrm{d}\theta \\ &- \left(\frac{1}{2} m v_\parallel^2 - \frac{1}{2} m u_0^2 + Ze\Phi(\mathbf{X}) + \mu B(\mathbf{X}) \right) \mathrm{d}t \ . \end{aligned} \tag{18}$$

Note that as a consequence of the Lagrangian being independent of the gyrophase θ, the magnetic moment μ (the associated conjugated coordinate pair of θ) becomes an invariant of the motion ($\dot{\mu} = 0$).

As in Chapter 3.2.1 perturbations [Eq. (6)] will get introduced to the guiding center Lagrangian. The transformation of the equilibrium part is already performed above, so only the pertrubation part with the pertubated Lagrangian in the particle phase space γ_1 has to be transfromed to the guiding center phase space. The transformation is analogous to the calculation before, the key difference is that the fluctuations quantities vary on a small length scale and Taylor expansion around the guiding center $\mathbf{X}$ can not be applied advantageous. Their values have to be taken at the particle position, which is a function of the gyroangle in guiding center coordinates. After this clearification the components of the perturbated Lagrangian in the guiding center phase space can be written as

$$\begin{aligned} \Gamma_{1,X^i} &= \gamma_{1,x^j} \frac{\mathrm{d}x^j}{\mathrm{d}X^i} & \Gamma_{1.v_\parallel} &= 0 \\ \Gamma_{1,\mu} &= \gamma_{1,x^j} \frac{\mathrm{d}x^j}{\mathrm{d}\mu} & \Gamma_{1,\theta} &= \gamma_{1,x^j} \frac{\mathrm{d}x^j}{\mathrm{d}\theta} \\ \Gamma_{1,t} &= \gamma_{1,t} \ . \end{aligned} \tag{19}$$

After inserting the components of the perturbated Lagrangian γ_1 and neglecting terms of order ρ^2, due to gyrokinetic ordering, the pertrubated compentents in the guiding center coordinates can be expressed as

$$\begin{aligned}
\Gamma_{1,\mathbf{X}} &\approx Ze\mathbf{A}_1(\mathbf{x}) & \Gamma_{1.v_\parallel} &= 0 \\
\Gamma_{1,\mu} &= \frac{Z}{|Z|}\frac{1}{v_\perp(\mathbf{X},\mu)}\mathbf{A}_1(\mathbf{x})\cdot\mathbf{a}(\theta) & \Gamma_{1,\theta} &= \frac{Z}{|Z|}\frac{2\mu}{v_\perp(\mathbf{X},\mu)}\mathbf{A}_1(\mathbf{x})\cdot\frac{\mathrm{d}\mathbf{a}(\theta)}{\mathrm{d}\theta} \\
\Gamma_{1,t} &= -Ze\Phi_1(\mathbf{x})\ .
\end{aligned} \tag{20}$$

Finally, the fundamental one-form in the guiding center phase space Γ with perturbation can be written as

$$\begin{aligned}
\Gamma &= \langle\Gamma_0\rangle + \Gamma_1 \\
\langle\Gamma_0\rangle &= \big(mv_\parallel\mathbf{b}(\mathbf{X}) + m\mathbf{u}_0 + Ze\mathbf{A}_0(\mathbf{X})\big)\cdot\mathrm{d}\mathbf{X} + \frac{2\mu m}{Ze}\mathrm{d}\theta \\
&\quad - \left(\frac{1}{2}mv_\parallel^2 - \frac{1}{2}mu_0^2 + Ze\Phi_0(\mathbf{X}) + \mu B_0(\mathbf{X})\right)\mathrm{d}t \\
\Gamma_1 &= Ze\mathbf{A}_1(\mathbf{x})\cdot\mathrm{d}\mathbf{X} + \frac{Z}{|Z|}\frac{1}{v_\perp}\mathbf{A}_1(\mathbf{x})\cdot\mathbf{a}\mathrm{d}\mu + \frac{Z}{|Z|}\frac{2\mu}{v_\perp}\mathbf{A}_1(\mathbf{x})\cdot\frac{\mathrm{d}\mathbf{a}}{\mathrm{d}\theta}\mathrm{d}\theta - Ze\Phi_1(\mathbf{x})\mathrm{d}t\ .
\end{aligned} \tag{21}$$

3.2.3 Lagrangian in Gyrocenter Phase Space

The transformation of the guiding center Lagrangian Γ into the Lagrangian in gyrocenter phase space $\bar{\Gamma}$ aims to remove the gyroangle θ dependence resulting from the introduction of fluctuations. To destinguish between the guiding center and the gyrocenter coordinates all quantities associated with the gyrocenter are getting an overbar, i.e. $\bar{\Gamma}$. The new set of gyrocenter coordinates are given by $\{\bar{\mathbf{X}}, \bar{v_\parallel}, \bar{\mu}\}$ but these coordinates will not been used in this thesis. Since the derivation of fundamental the one-form in gyrocenter phase space $\bar{\Gamma}$ uses the Lie transform pertubation method, which is beyond the scopes of this thesis, the reader is referred to the Refs. 4 and 19 for more details. The Lagrangian in the gyrocenter phase space can be expressed as

$$\begin{aligned}\bar{\Gamma} &= \bar{\Gamma}_0 + \bar{\Gamma}_1 \\ &= \left(mv_\parallel \mathbf{b}_0(\mathbf{X}) + m\mathbf{u}_0 + Ze\left(\mathbf{A}_0(\mathbf{X}) + \bar{\mathbf{A}}_1(\mathbf{X})\right)\right)\cdot \mathrm{d}\mathbf{X} + \frac{2\mu m}{Ze}\mathrm{d}\theta \\ &\quad - \left(\frac{1}{2}m\left(v_\parallel^2 - u_0^2\right) + Ze\left(\Phi_0(\mathbf{X}) + \bar{\Phi}_1(\mathbf{X})\right) + \mu\left(B_0(\mathbf{X}) + \bar{B}_{1\parallel}(\mathbf{X})\right)\right)\,\mathrm{d}t\ ,\end{aligned} \tag{22}$$

where B_0 is the equilibrium magnetic field and $\bar{B}_{1\parallel}$ is the magnetic field introduced by the vector potential $\mathbf{A}_1$. Note, that the quantities $\bar{\Phi}_1$, $\bar{\mathbf{A}}_1$ and $\bar{B}_{1\parallel}$ are the shorter notation of following gyroaveraged quantities defined as

$$\begin{aligned}\langle\Phi_1(\mathbf{x})\rangle &= J_0(\lambda)\Phi_1(\mathbf{X}) = \bar{\Phi}_1(\mathbf{X}) \\ \langle\mathbf{A}_1(\mathbf{x})\rangle &= J_0(\lambda)\mathbf{A}_1(\mathbf{X}) = \bar{\mathbf{A}}_1(\mathbf{X}) \\ Ze\langle\mathbf{A}_1(\mathbf{x})\cdot\mathbf{v}_\perp(\mathbf{X},\mu,\theta)\rangle &= -\hat{J}_1(\lambda)\mu B_{1\parallel}(\mathbf{X}) = \mu\bar{B}_{1\parallel}(\mathbf{X})\ .\end{aligned} \tag{23}$$

To obtain Equation (23) the particle coordinate $\mathbf{x}$ gets seperated gyrocenter coordinate $\mathbf{X}$ and the Larmor radius vector $\rho\mathbf{a}$ while express the gyroaveraged quantity in the Fourier space with the wave vector $\mathbf{k}$ defined as $\mathbf{k} = \hat{e}_1 k_\perp$. J_0 is the zeroth order Bessel function and $\hat{J}_1$ is a modified first order Bessel function of first kind defined as $\hat{J}_1(z) = 2/zJ_1(Z)$. The argument λ is given by $i\rho\nabla_\perp$ which is the inverse Fourier transformated expression of $\rho k_\perp$.

The components of the gyrocenter Lagrangian are again indepedent of the gyrophase θ, and therefore the teh magnetic moment μ remains in the gyrocenter pahse space an invariant of motion.

3.3 Gyrokinetic Equation

3.3.1 Vlasov Equation

Because of the large number of particles in the fusion plasma a prediction on the basis of Newton-Maxwell dynamics results in an impossible task for simulation, but this problem can be solved with a statistical approach. For that the distribution function $f(\mathbf{x}, \mathbf{v}, t)$ in the particle phase space $\{\mathbf{x}, \mathbf{v}\}$ will be considered. Because collisions are happening at much smaller frequencies than the characteristic frequencies connected to turbulence, the collisionless model is often preferred[7] which results through evolution of the particle density distribution function in the *Vlasov equation*

$$\frac{\partial f}{\partial t} + \dot{\mathbf{x}} \cdot \frac{\partial f}{\partial \mathbf{x}} + \dot{\mathbf{v}} \cdot \frac{\partial f}{\partial \mathbf{v}} = 0 \ . \tag{24}$$

In the gyrocenter phase space $\{\mathbf{X}, v_\parallel, \mu\}$. The overbar introduced in Chapter 3.2.3 gets droped for simplicity for all quantities. the Vlasov equation takes following form

$$\frac{\partial f}{\partial t} + \dot{\mathbf{X}} \cdot \frac{\partial f}{\partial \mathbf{X}} + \dot{v}_\parallel \cdot \frac{\partial f}{\partial v_\parallel} = 0 \ , \tag{25}$$

where the gyrophase θ is still an ignorable coordinate and the time derivative of the magnetic moment μ is zero, beacause the magnetic moment μ is an exact invariant. In Equation (25) the terms of the time derivative of the gyrocenter $\dot{\mathbf{X}}$ and the parallel velocity $\dot{v_\parallel}$ have to be expressed through the gyrocenter Lagrangian with the Euler-Lagrange equation. The Euler-Lagrange equation can be written as

$$\left(\frac{\partial \gamma_j}{\partial z^i} - \frac{\partial \gamma_i}{\partial z^j} \right) \frac{\mathrm{d}z^j}{\mathrm{d}t} = \frac{\partial H}{\partial z^i} + \frac{\partial \gamma_i}{\partial t} \ . \tag{26}$$

Inserting Equation (22) into the Euler-Lagrange equation and apply multiple calculations detailed in Ref. 19 the equations of motion can be obtained as

$$\begin{aligned} \dot{\mathbf{X}} &= v_\parallel \mathbf{b}_0 + \mathbf{v}_\chi + \mathbf{v}_\mathrm{D} \qquad & \dot{v}_\parallel &= \frac{\dot{\mathbf{X}}}{m v_\parallel} \cdot \Big(Ze\bar{\mathbf{E}} - \mu \nabla (B_0 + \bar{B}_{1\parallel}) + \underbrace{\frac{1}{2} m \nabla u_0^2}_{mR\Omega^2 \nabla R} \Big) \\ \dot{\mu} &= 0 & \dot{\theta} &= \omega_\mathrm{c} - \frac{Ze}{m} \partial_\mu \left(Ze\bar{\mathbf{A}}_1 \cdot \dot{\mathbf{X}} - Ze\bar{\Phi}_1 - \mu \bar{B}_{1\parallel} \right) \ , \end{aligned} \tag{27}$$

with the drift velocity $\mathbf{v}_\chi$ defined as the sum of the streaming velocity perpendicular to the pertubated magnetic field $\mathbf{v}_{\bar{B}_{1\perp}}$, the $\mathrm{E} \times \mathrm{B}$ drift in the total electric field $\mathbf{v}_{\bar{E}}$ and the grad-B dirft of the parallel perturbed magnetic field $\mathbf{v}_{\nabla \bar{B}_{1\parallel}}$. The drift velocity $\mathbf{v}_\mathrm{D}$ containing the sum of the curvature drift $\mathbf{v}_C$, the grad-B drift of the equilibrium

magnetic field $\mathbf{v}_{\nabla B_0}$ and the drifts due to the Coriolis force $\mathbf{v}_{\mathrm{Co}}$ and centrifugal force $\mathbf{v}_{\mathrm{Ce}}$. The quantity χ can be expressed as

$$\chi = \underbrace{(\Phi_0 + \bar{\Phi}_1)}_{\bar{\Phi}} - v_\parallel \bar{A}_{1\parallel} + \frac{\mu}{Ze} \bar{B}_{1\parallel} \tag{28}$$

with which follows the drift velocity $\mathbf{v}_\chi$

$$\mathbf{v}_\chi = \frac{\mathbf{b} \times \nabla \chi}{B_0} = \mathbf{v}_{\bar{B}_{1\perp}} + \mathbf{v}_{\bar{E}} + \mathbf{v}_{\nabla \bar{B}_{1\parallel}} \ . \tag{29}$$

Note that the term containing u_0^2 got replaced with Equation (12) with $u_0^2 = R^2\Omega^2$ and the total electric field $\bar{\mathbf{E}}$ is defined as

$$\bar{\mathbf{E}} = -\nabla \bar{\Phi} - \partial_t \bar{\mathbf{A}}_1 \approx -\nabla \bar{\Phi} - \partial_t \bar{\mathbf{A}}_{1\parallel} \ , \tag{30}$$

since the time derivative of the vector potential $\partial_t \bar{\mathbf{A}}_{1\perp}$ is one order smaller as the gradient of the electrostatic potential $\nabla \bar{\Phi}$ due to normalization assumptions in gyrokinetics(Source).

3.3.2 The delta-*f* Approximation

The delta-f approximation separates the density distrubution function f into an equilibrium part f_0 and pertubation part δf, i.e. $f = f_0 + \delta f$. Applying the delta-f approximation on the gyrocenter Vlasov equation leads to

$$\frac{\partial \delta f}{\partial t} + \dot{\mathbf{X}} \cdot \nabla \delta f + \dot{v}_\parallel \cdot \frac{\partial \delta f}{\partial v_\parallel} = \underbrace{-\dot{\mathbf{X}} \cdot \nabla f_0 - \dot{v}_\parallel \frac{\partial f_0}{\partial v_\parallel}}_{S} \ , \tag{31}$$

with the source term S. Substituting from Equation (27) the equations for $\dot{\mathbf{X}}$ and $\dot{v}_\parallel$ into the delta-f aproximated Vlasov equation results in

$$\frac{\partial \delta f}{\partial t} + \dot{\mathbf{X}} \cdot \nabla \delta f - \frac{\mathbf{b}_0}{m} \cdot \left(Ze \nabla \Phi_0 + \mu \nabla B_0 - mR\Omega^2 \nabla R \right) \cdot \frac{\partial \delta f}{\partial v_\parallel} = S \ . \tag{32}$$

Note that only the terms of order $\rho_\star$ has to be kept in $\dot{v}_\parallel \partial_{v_\parallel} \delta f$, which results in neglecting the drift velocities $\mathbf{v}_\chi$ and $\mathbf{v}_\mathrm{D}$ and the contribution of $\bar{B}_{1\parallel}$ and $\bar{\Phi}_1$, since these terms are after calculation of order $\rho_\star^2$.

The equilibrium distribution fuction f_0 is assumed to be a Maxwellian which includes a finite equilibrium electric field Φ_0 to balance the centrifugal force (in the co-rotating frame) due toridial rotation of the plasma. In the rotating frame the included term can be written as(Source)

$$\mathcal{E} = Ze\langle \Phi_0 \rangle - \frac{1}{2} m \omega_\varphi^2 \left(R^2 - R_0^2 \right) \ , \tag{33}$$

where $\langle \cdot \rangle$ denote flux-surface averaging, ω_φ the plasma rotation frequency [Eq. (13)], R the local major radius and R_0 is an integration constant which can be chosen, i.e. major radius of the plasma or flux surface average of the major radius(Source). The Maxwellian is given by the following expression

$$f_0 = F_\mathrm{M}(\mathbf{X}, v_\parallel, \mu) = \frac{n_0}{(2\pi T/m)^{3/2}} \exp\left(-\frac{\frac{1}{2} m (v_\parallel - u_\parallel)^2 + \mu B_0 + \mathcal{E}}{T} \right) \ , \tag{34}$$

where n_0 is the equilibrium particle density and $u_\parallel$ is the rotation speed of the plasma in the rotating frame parallel to the magnetic field [Eq. (14)]. The derivatives of the Maxwellian can be expressed as(Source)

$$\begin{aligned} \nabla F_\mathrm{M} = & \left[\frac{\nabla n_0}{n_0} + \left(\frac{\frac{1}{2} m v_\parallel^2 + \mu B_0 + \mathcal{E}}{T} - \frac{3}{2} \right) \frac{\nabla T}{T} - \frac{\mu B_0}{T} \frac{\nabla B_0}{B_0} \right. \\ & \left. + \left(\frac{m v_\parallel R B_\mathrm{t}}{BT} + m\omega \left(R^2 - R_0^2 \right) \right) \nabla \omega_\varphi \right] F_\mathrm{M} \\ \partial_{v_\parallel} F_\mathrm{M} = & -\frac{m v_\parallel}{T} F_\mathrm{M} \\ \partial_\mu F_\mathrm{M} = & -\frac{B_0}{T} F_\mathrm{M} \ , \end{aligned} \tag{35}$$

where the $\nabla\omega_\varphi$ terms are the result of the derivatives of the parallel rotation velocity $u_\parallel$ and rotation energy $\mathcal{E}$ evaluated at zero rotation speed locally in the co-rotating frame. It can be shown with Equations (27) and (35) that the ∇B_0 term in $-\dot{\mathbf{X}} \cdot \nabla F_\mathrm{M}$ cancels with $(\dot{\mathbf{X}}/mv_\parallel)\mu\nabla B_0\partial_{v_\parallel} F_\mathrm{M}$ for purely torodial rotation. Finally, the source term can than be written as

$$\begin{aligned} S = &-(\mathbf{v}_\chi + \mathbf{v}_\mathrm{D}) \cdot \tilde{\nabla} F_\mathrm{M} - \frac{Zev_\parallel}{T}\partial_t \bar{A}_{1\parallel} F_\mathrm{M} \\ &-\frac{F_\mathrm{M}}{T}(v_\parallel \mathbf{b}_0 + \mathbf{v}_\mathrm{D} + \mathbf{v}_{\bar{B}_{1\perp}}) \cdot (Ze\nabla\bar{\Phi} + \mu\nabla\bar{B}_{1\parallel}) \ , \end{aligned} \tag{36}$$

where $\tilde{\nabla}$ referres to only the ∇n_0, ∇T and $\nabla\omega_\varphi$ terms of ∇F_M.

3.4 Gyrokinetic Field Equations

3.4.1 Maxwell's Equations

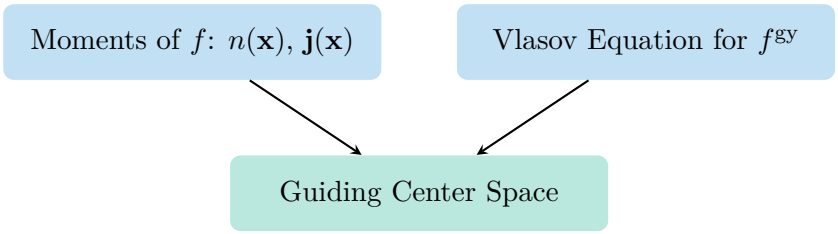

Figure 3.3: Idea of gyrokinetic Maxwell's equations: The particle density $n(\mathbf{x})$, the current density $\mathbf{j}(\mathbf{x})$ and the gyrocenter distribution function f^{gy} are expressed in th guiding center phase space.

To obtain a closed system the Vlasov equation gets combined with the Maxwell equations. The particle density n and current density j can be described with the distribution function f as follows

$$n = \int \mathrm{d}\mathbf{v}\, f(\mathbf{x}, \mathbf{v}, t) \qquad j = q \int \mathrm{d}\mathbf{v}\, v f(\mathbf{x}, \mathbf{v}, t)\ , \tag{37}$$

which are then substituted into the Maxwell equations

$$\begin{aligned} \nabla \cdot \mathbf{B} &= 0 & \nabla \times \mathbf{B} &= \mu_0 \left(\sum_{\text{species}} j + \epsilon_0 \frac{\partial \mathbf{E}}{\partial t} \right) \\ \nabla \cdot \mathbf{E} &= \frac{1}{\epsilon_0} \sum_{\text{species}} qn & \nabla \times \mathbf{E} &= -\frac{\partial \mathbf{B}}{\partial t}\ . \end{aligned} \tag{38}$$

The Vlasov equation (24) in combination with the Maxwell equations (37) and (38) is the basis of the gyrokinetic model. [10]

3.5 Electromagnetic Gyrokinetic Models in GKW

Global Gyrokinetic simulations are suffering from nummerical problems, mainly from the cancellation problem examined codes which uses the paticle-in-cell or the Eulerian methods. (Source)This problem limits the electromagnetic investigations to extremely low β parameters. As in Chapter 3.3.2 discussed gets the density distribution function f seperated into an equilibrium part f_0, i.e. a Maxwellian F_M, and a pertrubated part δf. This seperation results in the appearence of the term of the pertrubed vector potential $\bar{A}_{1\|}$ in the Source term [Eq. (36)] which is computationally difficult to evaluate. To avoid further complications a modified distribution function g will be introduced as

$$g = \delta f + \frac{Zev_\|}{T}\bar{A}_{1\|}F_\mathrm{M} \ . \tag{39}$$

Substituting the modified distribution function g into Equation (32) results in

$$\frac{\partial g}{\partial t} + \mathbf{v}_\chi \cdot \nabla g + (v_\| \mathbf{b}_0 + \mathbf{v}_\mathrm{D}) \cdot \nabla \delta f - \frac{\mathbf{b}_0}{m} \cdot (Ze\nabla\Phi_0 + \mu\nabla B_0 - mR\Omega^2\nabla R)\frac{\partial \delta f}{\partial v_\|} = S \tag{40}$$

$$S = -(\mathbf{v}_\chi + \mathbf{v}_\mathrm{D}) \cdot \tilde{\nabla} F_\mathrm{M} + \frac{F_\mathrm{M}}{T}(v_\| \mathbf{b}_0 + \mathbf{v}_\mathrm{D}) \cdot (-Ze\nabla\bar{\Phi}_1 - \mu\nabla\bar{B}_{1\|}) \ . \tag{41}$$

This is the form of the Vlasov equation currently implemented in GKW(Source). The goal of this Chapter is to handle the $\partial_t \bar{A}_{1\|}$ term with the consideration of electromagnetic fields and rework the Vlasov equation and Maxwell's equations for GKW. This section follows the work of P.C. Crandall in his Disseration[3].

3.5.1 Introduction of the Induktive Field $E_\|$

First the Vlasov equation gets written down in the δf framework with the source term [Eq. (32) & (36)] will get simplified into

$$\frac{\partial \delta f}{\partial t} - \frac{Zev_\|}{T}\partial\bar{A}_{1\|}F_\mathrm{M} = R \ , \tag{42}$$

where R represents all terms which excludes the plasma induction $\partial_t \bar{A}_{1\|}$. The equation of the $\bar{A}_{1\|}$ is given by

$$\nabla \mathbf{A}_{1\|} = -\mu \mathbf{j}_{1\|} \ . \tag{43}$$

CHAPTER

4 Bibliography

[1] Barton, Justin E., Wehner, William P., Schuster, Eugenio, Felici, Federico & Sauter, Olivier 2015 Simultaneous closed-loop control of the current profile and the electron temperature profile in the tcv tokamak. URL `https://ieeexplore.ieee.org/document/7171844`.

[2] Brizard, A. J. & Hahm, T. S. 2007 Foundations of nonlinear gyrokinetic theory. *Rev. Mod. Phys.* **79**, 421–468.

[3] Crandall, P.C. 2019 *Collisional and Electromagnetic Physics in Gyrokinetic Models*. PhD thesis, University of Carlifornia Los Angeles.

[4] Dannert, T. 2005 *Gyrokinetische Simulation von Plasmaturbulenz mit gefangenen Teilchen und Elektromagnetischen Effekten*. PhD thesis, Technische Universtät München.

[5] Dif-Pradalier, G., Diamond, P. H., Grandgirard, V., Sarazin, Y., Abiteboul, J., Garbet, X., Ghendrih, Ph., Strugarek, A., Ku, S. & Chang, C. S. 2010 On the validity of the local diffusive paradigm in turbulent plasma transport. *Phys. Rev. E* **82**, 025401.

[6] Dif-Pradalier, G., Hornung, G., Ghendrih, Ph., Sarazin, Y., Clairet, F., Vermare, L., Diamond, P. H., Abiteboul, J., Cartier-Michaud, T., Ehrlacher, C., Estève, D., Garbet, X., Grandgirard, V., Gürcan, Ö. D., Hennequin, P., Kosuga, Y., Latu, G., Maget, P., Morel, P., Norscini, C., Sabot, R. & Storelli, A. 2015 Finding the elusive E×B staircase in magnetized plasmas. *Phys. Rev. Lett.* **114**, 085004.

[7] Garbet, X., Idomura, Y., Villard, L. & Watanabe, T. H. 2010 Gyrokinetic simulations of turbulent transport. *Nuclear Fusion* **50** (4).

[8] Kim, Y. J., Imadera, K., Kishimoto, Y. & Hahm, T. S. 2022 Transport events and E×B staircase in flux-driven gyrokinetic simulation of ion temperature gradient turbulence. *Journal of the Korean Physical Society* **81**, 636.

[9] Kishimoto, Y., Imadera, K., Ishizawa, A., Wang, W. & Li, J. Q. 2023 Characteristics of constrained turbulent transport in flux-driven toroidal plasmas. *Philosophical Transactions of the Royal Society A: Mathematical, Physical and Engineering Sciences* **381** (2242), 20210231.

[10] Krommes, John A. 2012 The Gyrokinetic Description of Microturbulence in Magnetized Plasmas. *Annual Review of Fluid Mechanics* .

[11] Krommes, John A. & Kim, Chang-Bae 2000 Interactions of disparate scales in drift-wave turbulence. *Phys. Rev. E* **62**, 8508–8539.

[12] McMillan, B. F., Jolliet, S., Tran, T. M., Villard, L., Bottino, A. & Angelino, P. 2009 Avalanchelike bursts in global gyrokinetic simulations. *Phys. of Plasmas* **16** (2), 022310.

[13] Peeters, A. G., Rath, F., Buchholz, R., Camenen, Y., Candy, J., Casson, F. J., Grosshauser, S. R., Hornsby, W. A., Strintzi, D. & Weikl, A. 2016 Gradient-driven flux-tube simulations of ion temperature gradient turbulence close to the non-linear threshold. *Phys. of Plasmas* **23** (8), 082517.

[14] Peeters, A. G., Strintzi, D., Camenen, Y., Angioni, C., Casson, F. J., Hornsby, W. A. & Snodin, A. P. 2009 Influence of the centrifugal force and parallel dynamics on the toroidal momentum transport due to small scale turbulence in a tokamak. *Phys. of Plasmas* **16** (4), 042310.

[15] Rath, F., Peeters, A. G. & Weikl, A. 2021 Analysis of zonal flow pattern formation and the modification of staircase states by electron dynamics in gyrokinetic near marginal turbulence. *Phys. of Plasmas* **28** (7), 072305.

[16] Seiferling, F., Peeters, A. G., Grosshauser, S. R., Rath, F. & Weikl, A. 2019 The interplay of an external torque and e×b structure formation in tokamak plasmas. *Phys. of Plasmas* **26** (10), 102306.

[17] Seo, Janghoon, Jhang, Hogun & Kwon, Jae-Min 2022 Effects of light impurities on zonal flow activities and turbulent thermal transport. *Phys. of Plasmas* **29** (5), 052502.

[18] Stroth, Ulrich 2011 *Plasmaphysik*. Wiesbaden: Viewg+Teubner.

[19] Szepesi, Gábor 2023 Derivation of the fully electro-magnetic, non-linear, gyrokinetic vlasov–maxwell equations in a rotating frame of reference for gkw with lie transform perturbation method. unpublished. URL `https://bitbucket.org/gkw/gkw/src/develop/doc/etc/derivation.tex`.

[20] Villard, L, Angelino, P, Bottino, A, Brunner, S, Jolliet, S, McMillan, B F, Tran, T M & Vernay, T 2013 Global gyrokinetic ion temperature gradient turbulence simulations of iter. *Plasma Physics and Controlled Fusion* **55** (7), 074017.

[21] Wang, W., Kishimoto, Y., Imadera, K., Liu, H.R., Li, J.Q., Yagi, M. & Wang, Z.X. 2020 Statistical study for itg turbulent transport in flux-driven tokamak plasmas based on global gyro-kinetic simulation. *Nuclear Fusion* **60** (6), 066010.

[22] Weikl, A., Peeters, A. G., Rath, F., Grosshauser, S. R., Buchholz, R., Hornsby, W. A., Seiferling, F. & Strintzi, D. 2017 Ion temperature gradient turbulence close to the finite heat flux threshold. *Phys. of Plasmas* **24** (10), 102317.

[23] Wesson, John 2011 *Tokamaks*. Oxford: Oxford University Press.

Eidesstattliche Erklärung

Hiermit erkläre ich, Manuel Lippert, dass ich die vorliegende Arbeit selbständig und ohne Benutzung anderer als der angegebenen Hilfsmittel angefertigt habe. Alle Stellen,

die wörtlich oder sinngemäß aus veröffentlichten oder nicht veröffentlichten Schriften entnommen wurden, sind als solche kenntlich gemacht. Die Arbeit hat in gleicher oder

ähnlicher Form noch keiner anderen Prüfungsbehörde vorgelegen.

Bayreuth, den 30.06.2023

Manuel Lippert